Peer-reviewed version available at *Universe* **2017**, *3*, 9; doi:10.3390/universe3010009

Article

Initial Energy Density of $\sqrt{s} = 7$ and 8 TeV p+p Collisions at the LHC

Máté Csanád [1], Tamás Csörgő [2,3], Ze-Fang Jiang [4] and Chun-Bin Yang [4]

1 Eötvös Loránd University, H – 1117 Budapest, Pázmány P. s. 1/A, Hungary
2 Wigner RCP, H – 1525 Budapest 114, POBox 49, Hungary
3 EKU KRC, H – 3200 Gyöngyös, Mátrai út 36
4 Central China Normal Universit, 152 Luoyu Road ,Wuhan, Hubei 430079, People's Republic of China
* Correspondence: csanad@elte.hu

Abstract: Accelerating, exact, explicit and simple solutions of relativistic hydrodynamics allow for a simple and natural description of highly relativistic p+p collisions. These solutions yield a finite rapidity distribution, thus they lead to an advanced estimate of the initial energy density of high energy collisions. We show that such an advanced estimate yields an initial energy density in $\sqrt{s} = 7$ and 8 TeV p+p collisions at LHC around the critical energy density from lattice QCD, and a corresponding initial temperature around the critical temperature from QCD and the Hagedorn temperature. The multiplicity dependence of the estimated initial energy density suggests that in high multiplicity pp collisions at the LHC, there is large enough initial energy density to create a non-hadronic perfect fluid.

Keywords: quark-gluon plasma, hydrodynamics, pseudorapidity distribution, initial state, energy density, Bjorken estimate

PACS: 25.75.-q,25.75.Nq,13.85.-t

1. Introduction

The interest in relativistic hydrodynamics grew in past years mainly due to the discovery of the nearly perfect fluidity of the experimentally created Quark-Gluon-Plasma (QGP) at the Relativistic Heavy Ion Collider (RHIC) [1]. Hydrodynamical models aim to describe the space-time picture of heavy-ion collisions and infer the relation between experimental observables and the initial conditions. Besides numerical simulations there is also an interest in models where exact solutions of the hydrodynamical equations are used. It is customary to describe the medium created in heavy ion collisions with hydrodynamic models, however, the proton-proton system is frequently considered as a system that might be too small for thermalization, or that might be not hot or dense enough to create a supercritical (non-hadronic) medium. Energy densities in $\sqrt{s} = 200$ GeV p+p collisions are likely below this limit. It is however an interesting question, how high energy densities can be reached in p+p collisions at the LHC with $\sqrt{s} = 7$ and higher collision energies. In this paper we apply the hydrodynamical solution of Refs. [2,3] to describe the pseudorapidity distribution in pp collisions at $\sqrt{s} = 7$ and 8 TeV and use the results of these hydrodynamical fits to estimate the initial energy density in these reactions.

2. Hydrodynamics

The basic hydrodynamical equations are the continuity and energy-momentum-conservation equations:

$$\partial_\nu (n u^\nu) = 0, \qquad \partial_\nu T^{\mu\nu} = 0, \tag{1}$$

Peer-reviewed version available at Universe 2017, 3, 9; doi:10.3390/universe3010009

with n being a conserved charge, and T is the energy-momentum tensor. In case of a perfect fluid

$$T^{\mu\nu} = (\epsilon + p)u^\mu u^\nu - pg^{\mu\nu}. \tag{2}$$

where ϵ is the energy density and p the pressure. The Equation of State (EoS) closes the set of equations: $\epsilon = \kappa p$ while $p = nT$ defines temperature T. An analytic hydrodynamical solution is a functional form of ϵ, p, T, u^μ and n, which solves the above equations. The solution is explicit if these fields are explicitly given as a function of space-time coordinates $x^\mu = (t, \mathbf{r}) = (t, r_x, r_y, r_z)$, or in a general d-dimensional case, $x^\mu = (t, r_1, \ldots, r_d)$.

We discuss the solution detailed in Refs. [2–5]:

$$u^\mu = (\mathrm{ch}\lambda\eta, \mathrm{sh}\lambda\eta),\ n = n_f \frac{\tau_f^\lambda}{\tau^\lambda},\ T = T_f \left(\frac{\tau_f}{\tau}\right)^{\frac{\lambda}{\kappa}}. \tag{3}$$

Here $\tau = \sqrt{t^2 - \mathbf{r}^2}$ is a coordinate proper-time, $\eta = 0.5\sqrt{(t + |\mathbf{r}|)/(t - |\mathbf{r}|)}$ the space-time rapidity, subscript f denotes quantities at the freeze-out, while λ controlls the acceleration. If $\lambda = 1$ (and the expansion is one-dimensional), there is no acceleration and we get back the accelerationless Hwa-Bjorken solution of Ref. [6,7]. However, Refs. [2–5] described one-dimensional hydrodynamical solutions for any real value of λ, for the special EoS of $\kappa = 1$.

3. Rapidity distributions

The differential rapidity distribution or rapidity density dN/dy (with N being then the total number of particles) was calculated in Refs. [2–5]:

$$\frac{dN}{dy} \approx N_0 \cosh^{\frac{\alpha}{2}-1}\left(\frac{y}{\alpha}\right) e^{-\frac{m}{T_f}\cosh^\alpha\left(\frac{y}{\alpha}\right)}, \tag{4}$$

with $\alpha = \frac{2\lambda-1}{\lambda-1}$, and N_0 is a normalization parameter.

The rapidity distribution is approximately Gaussian, if $\lambda > 1$. At $\lambda = 1$, the distribution becomes flat, as in this is the Bjorken limit (corresponding to the Hwa-Bjorken solution), the solution becomes boost invariant. Also note that in order to describe experimental data, pseudorapidity distributions have to be calculated as well. See details in Refs. [2–5].

4. Energy density estimation

In this section we recapitulate how this model can be used for improving the famous energy density estimation made by Bjorken [7]. Let us focus on the thin transverse slab at mid-rapidity, just after thermalization ($\tau = \tau_0$), illustrated by Fig. 2 of Ref. [7]. The radius R of this slab is estimated by the radius of the colliding hadrons or nuclei, and the initial "fireball" volume is $dV = (R^2\pi)\tau_0 d\eta_0$, where $\tau_0 d\eta_0$ is the longitudinal size, as $d\eta_0$ is the pseudorapidity width at τ_0. See Refs. [2–5] for details. The energy content is $dE = \langle E\rangle dN$, where dN is the number of particles and $\langle E\rangle$ is their average energy near $y = 0$. So, as given in Bjorken's paper, the initial energy density is for a boost invariant solution, we obtain Bjorken's energy density estimation as

$$\epsilon_{\mathrm{Bj}} = \frac{\langle E\rangle dN}{(R^2\pi)\tau_0 d\eta_0} = \frac{\langle E\rangle}{(R^2\pi)\tau_0}\left.\frac{dN}{d\eta}\right|_{\eta=\eta_0}. \tag{5}$$

Here τ_0 is the proper-time of thermalization, estimated by Bjorken as $\tau_0 \approx 1$fm.

For accelerationless, boost-invariant Hwa-Bjorken flows $\eta_0 = \eta_f = y$, however, for accelerating solutions one has to apply a correction to take into account the acceleration effects on the energy

density estimation [4]. Thus for the hydrodynamical solutions where the acceleration parameter is $\lambda > 0$. the initial energy density is given by a corrected estimation $\epsilon_{\rm corr}$ as

$$\epsilon_{\rm corr} = \epsilon_{\rm Bj} \left(2\lambda - 1\right) \left(\frac{\tau_f}{\tau_0}\right)^{\lambda - 1} \tag{6}$$

Here $\epsilon_{\rm Bj}$ is the Bjorken estimation, which is recovered if dN/dy is flat (i.e. $\lambda = 1$), but for $\lambda > 1$, both correction factors are bigger than 1. Hence the initial energy densities are under-estimated by the Bjorken formula, if the measured dn/dy distributions are not constant, but have a finite width. In Refs. [2–5] we performed fits to BRAHMS pseudo-rapidity distributions from Ref. [8], and these fits indicate that $\epsilon_{\rm corr} = 8.5 - 10$ GeV/fm^3 in $\sqrt{s_{\rm NN}} = 200$ GeV Au+Au collisions at RHIC.

The above corrections are exact results, that were derived in details for a special equation of state (EoS) of $\kappa = 1$ [4]. The correction factors in Eq. (6) take into account the work done by the pressure on the surface of a finite and accelerating, hot fireball. However, the relation of the pressure to the energy density is obviously EoS dependent, and as proposed in Refs. [2,3,5] the effects of a non-ideal equation of state can be estimated with the following formula:

$$\epsilon_{\rm corr} = \epsilon_{\rm Bj} \left(2\lambda - 1\right) \left(\frac{\tau_f}{\tau_0}\right)^{\lambda - 1} \left(\frac{\tau_f}{\tau_0}\right)^{(\lambda-1)(1-c_s^2)} \tag{7}$$

This conjecture satisfies several consistency requirements, for example, it goes back to the exact result of Eq. (6) in case of a super-hard EoS of $c_s = 1$ and gives initial energy density values that were checked against numerical solutions [2].

From basic considerations [7], as well as from lattice QCD calculations [9], it follows that the critical energy density, needed to form a non-hadronic medium is around 1 GeV/fm^3. From the lattice QCD calculations one gets $\epsilon_{\rm crit} = (6 - 8) \times T_{\rm crit}^4$ (in $\hbar c = 1$ units), and even with a conservative estimate of $T_{\rm crit} = 170$ MeV, one gets $\epsilon_{\rm crit} < 1$ GeV/fm^3. Thus initial energy densities above this value indicate the formation of a non-hadronic medium.

5. Initial energy densities in 7 and 8 TeV LHC p+p collisions

Let us estimate the quantities in Eq. (5). The average transverse momentum in $\sqrt{s} = 7$ TeV p+p collisions is $\langle p_t \rangle = 0.545 \pm 0.005_{\rm stat} \pm 0.015_{\rm syst}$ GeV/c [10], which corresponds to $\langle E \rangle = 0.562$ GeV/c^2 at midrapidity (assuming most of these particles are pions).

It is a non-trivial question, how to estimate the initial transverse area $R^2\pi$ in p+p collisions, because the geometrical area relates to the total, elastic, inelastic and differential cross-sections in an involved and non-trivial manner. In case of the collisions of large heavy ions, the initial overlap area is evaluated based on nuclear density profiles, for example using the relation $R \propto A^{1/3}$. Basically these relations that determine the nuclear geometry were obtained from the analysis of the differential cross-sections of elastic electron-ion [11] and elastic proton-nucleus data [12]. Similarly, to get a reliable estimate of the initial transverse area in p+p collisions, we should rely on the analysis of elastic p+p scattering data.

Our analysis is based on Eqs. (117-119) and (124-126) of Ref. [13], that show that both for a grey disc and for a Gaussian scattering density profile, $\sigma_{\rm el} = \pi R^2 A^2$ and $\sigma_{\rm tot} = 2\pi R^2 A$, where A measures the "greyness" of the proton. Thus the geometrical area $R^2\pi$ actually can be estimated as

$$\pi R^2 = \frac{\sigma_{\rm tot}}{2A} = \frac{\sigma_{\rm tot}^2}{4\sigma_{\rm el}}. \tag{8}$$

We have cross-checked these estimates by evaluating the geometrical area from B, the slope of differential elastic scattering cross-section at zero momentum transfer, as we may also use the relation $R^2\pi = 4\pi B$ [13]. We found that within errors both methods yield the same estimate for the initial

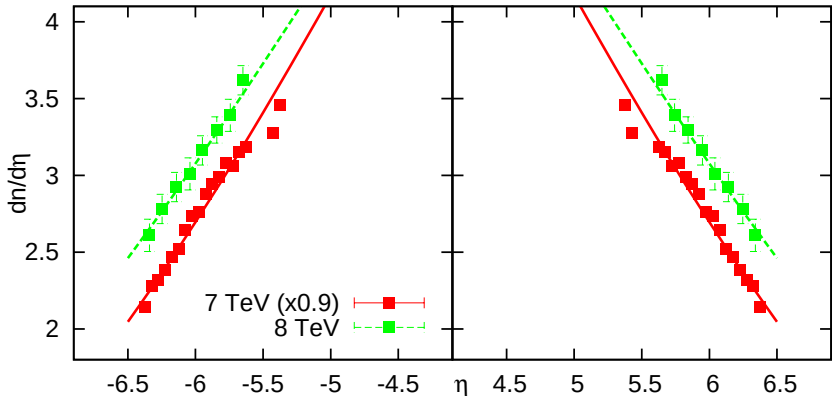

Figure 1. Charged particle $\frac{dN}{d\eta}$ distributions from TOTEM fitted with the result of the relativistic hydro solution described in this paper.

geometry of p+p collisions. Based on the results of Refs. [14,15], we have conservatively estimated $R = 1.76 \pm 0.02$ fm.

Furthermore, the formation time, τ_0, may conservatively assumed to be 1 fm/c. The only remaining parameter is the pseudorapidity density at midrapidity. As measured by the LHC experiments, the charged particle pseudorapidity density at midrapidity ($dn/d\eta|_{\eta=0}$) is found to be $6.01 \pm 0.01(\text{stat})^{+0.20}_{-0.12}(\text{syst})$ at ALICE [10], while $5.78 \pm 0.01_{\text{stat}} \pm 0.23_{\text{syst}}$ at CMS [16], but in some multiplicity classes it may reach values of 25-30 (see Table I. of Ref. [17]). We will take the average of the first two values. The total multiplicity is then $3/2\times$ the charged particle multiplicity. Substituting $1.5 dn/d\eta|_{\eta=0}$, based on Eq. (5) one gets:

$$\epsilon_{Bj}(7\text{ TeV}) = \frac{0.562 \times 1.5 \times 5.89}{1.76^2 \pi}\ \text{GeV/fm}^3 = 0.507\ \text{GeV/fm}^3, \tag{9}$$

which is below the critical value.

The advanced estimate is based on TOTEM pseudorapidity density $dN/d\eta$ data, as these reach out to large enough η values so that the acceleration parameter can be determined. Fits to TOTEM data were performed via Eq. (4) , as shown in Fig. 1. The fit resulted in the acceleration parameter $\lambda = 1.073 \pm 0.001_{\text{stat}} \pm 0.003_{\text{syst}}$, where the systematic error is based on the point-to-point systematic error of the data points.

Assuming $c_s^2 = 0.1$ (this is a quite realistic value, at least no harder EoS is expected at LHC, as similar EoS was found at RHIC as well [9,18,19]), one only needs a τ_f value. As shown in Eq. (3), temperature is proportional to $\tau^{-\lambda/\kappa}$. From this, $\tau_0 = \tau_f (T_f/T_0)^{\kappa/\lambda}$. Thus if the freeze-out temperature (assumed to be around the Hagedorn-temperature or the critical temperature of lattice QCD) is $T_f = 140$ MeV, then an initial temperature of $T_0 = 170$ MeV (needed in order to form a strongly interacting quark gluon plasma) corresponds to τ_f being 5-6 times τ_0, for $c_s^2 = 0.1$ and $\lambda = 1.1$. Even if c_s^2 and λ are higher, τ_f/τ_0 seems to be a rather conservative value. With this, one gets the multiplicative correction factors of 1.146 and 1.101, thus

$$\epsilon_{\text{corr}}(7\text{ TeV}) = 1.262 \epsilon_{\text{Bj}}(7\text{ TeV}) = 0.640\ \text{GeV/fm}^3 \tag{10}$$

which is still below the critical value. The c_s^2 and τ_f/τ_i dependence of the correction factor is shown in Fig. 2.

Note that the average p+p multiplicity was used here, so this value represents an average energy density in p+p collisions – below the critical value of 1 GeV/fm^3 (c.f. Ref [20] where a possible cross-over starting at $dn/d\eta|_{\eta=0} = 6$ was conjectured). Based on Table I. of Ref. [17], much larger multiplicities have been reached however. The energy density results for these multiplicities is

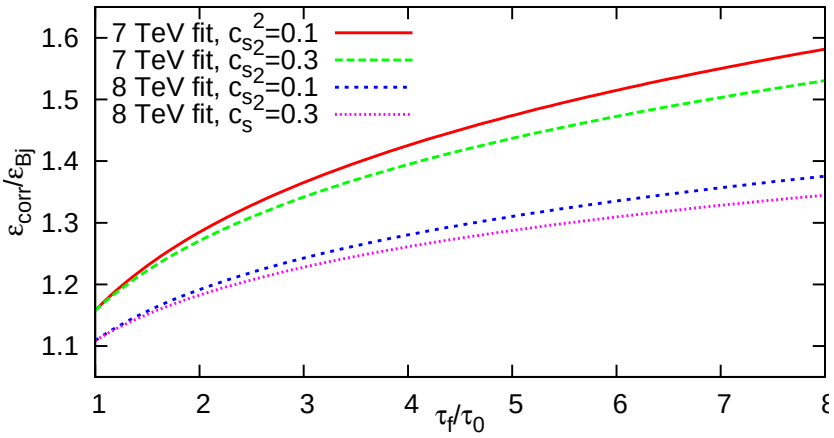

Figure 2. The correction factor as a function of freeze-out time versus thermalization time (τ_f/τ_0). At a reasonable value of 2, the correction factor is around 25%.

shown on Fig. 3. It is clear from this plot, that even for the original Bjorken estimate, supercritical enegy densities may have been reached in high multiplicity events, roughly from $dn/d\eta|_{\eta=0} \approx 12$. The corrected estimate gives supercritical values for $dn/d\eta|_{\eta=0} \approx 9$. We also calculated the initial temperature based on the $\epsilon \propto T^4$ relationship, assuming that 175 MeV corresponds to 1 GeV/fm^3 approximately. This is also shown in the left panel of Fig. 3, as well as the reachable pressure values. A temperature of 300-600 MeV may have been reached in 200 GeV central Au+Au collisions of RHIC [21]. Initial temperature values in 7 TeV p+p seem to be lower than that, 300 MeV can be reached in events with a multiplicity of > 50. However, 200 MeV may already be reached in events with a multiplicity of 16.

Now let us estimate what happens at $\sqrt{s} = 8$ TeV. As for the Bjorken-estimate, we need the change in charged particle multiplicity, average transverse energy and transverse size. CMS indicates $dn/d\eta|_{\eta=0} = 6.20 \pm 0.46$ for a non-single diffractive enhanced data sample in Ref. [22], while $dn/d\eta|_{\eta=0} = 6.13 \pm 0.1$ is given in Ref. [23]. The average of the two values is in good agreement with the approximate s dependence of $dn/d\eta|_{\eta=0}$ of $0.715 \cdot \sqrt{s}^{0.23}$ as estimated in Ref. [24]. Average transverse momentum s dependence is estimated as $\langle p_t \rangle = 0.413 - 0.0171 \ln s + 0.00143 \ln^2 s$ in Ref. [10], which means a 1.53% increase in $\langle E \rangle$. Transverse size can be estimated based on the $\sigma_{\rm tot}$ measurement of Refs. [25], $\sigma_{\rm tot} = 101.7 \pm 2.9(\text{syst})$ mb, which means a 3.8% increase in area compared to 7 TeV, and $R = 1.799 \pm 0.025$ fm Based on Eq. (5), this altogether means a 2.4% increase in $\epsilon_{\rm Bj}$, i.e.

$$\epsilon_{Bj}(8\text{ TeV}) = \frac{0.571 \times 1.5 \times 6.165}{1.799^2 \pi}\ \text{GeV/fm}^3 = 0.519\ \text{GeV/fm}^3, \tag{11}$$

which is again below the critical value. We also fitted $dN/d\eta$ data from TOTEM [22] as shown in Fig. 1. We obtained $\lambda = 1.067 \pm 0.001$ in this case. This corresponds to a correction factor of 1.240, similarly to Eq. (10). Finally, we arrive at

$$\epsilon_{\rm corr}(8\text{ TeV}) = 1.240 \times \epsilon_{\rm Bj}^{8\text{ TeV}} = 0.644\ \text{GeV/fm}^3. \tag{12}$$

This value is based on the average multiplicity in $\sqrt{s} = 8$ TeV collisions. However, at a fixed multiplicity, there is almost no difference between the two collision energies: average transverse energy increases by 1.5%, but the transverse also increases by 2.4%. This means a roughly 1% decrease, which is much smaller than the systematic uncertainties in this estimate – to be discussed in the next section. We plot the multiplicity dependence of $\epsilon_{\rm ini}$, $T_{\rm ini}$ and $p_{\rm ini}$ for the 8 TeV case in the right panel of Fig. 3. We may again observe, that supercritical values are reached for multiplicities

Table 1. Sources of statistical and systematic errors for the 7 TeV estimate.

parameter	value	stat.	syst. eff. on ϵ
λ	1.073	0.1%	0.4% (from data)
c_s^2	0.1	-	-2%+0.2% (if $0.05 < c_s^2 < 0.5$)
τ_f/τ_0	2	-	-4%+10% (for τ_f/τ_0 in 1.5–4)
τ_0 [fm/c]	1	-	underestimates ϵ
R [fm]	1.766	-	1.3% (from $\sigma_{\rm tot}$)
$\langle E\rangle$ [GeV/c^2]	0.562	0.5%	3%
$dN/d\eta$ (7 TeV)	5.895	0.2%	3%

higher than 10 in case of the corrected estimate; but even Bjorken's estimate yields supercriticality if $dn/d\eta|_{\eta=0} > 13$.

6. Uncertainty of the estimate

Different sources of uncertainties are detailed in Table 1. The most important one comes from $dn/d\eta$ at midrapidity. From Fig. 3 it is clear that for the Bjorken-estimate, energy density is above the critical value of 1 GeV/fm^3 if the multiplicity is larger than 12, while in case of the corrected initial energy density, $dn/d\eta|_{\eta=0} > 9$ is needed. Taking all sources of uncertainties into account, the final result for the energy density corresponding to mean multiplicity density at 7 TeV is

$$\epsilon_{\rm corr}(7\ {\rm TeV}) = 0.64 \pm 0.01({\rm stat})^{+0.14}_{-0.10}({\rm syst})\ {\rm GeV/fm}^3 \tag{13}$$

and the main systematic error comes from the estimation of the ratio τ_f/τ_0. In the 8 TeV case, the estimate yields a somewhat larger number (0.644 versus 0.640 GeV/fm^3), but the uncertainties are somewhat higher due to extrapolations to 8 TeV.

An important source of systematic uncertainty is the use of the given hydrodynamic solution. This uncertainty may be estimated by using other hydrodynamic models that contain acceleration: the Landau model [26], the Bialas-Peschanski model [27], or numeric models of hydrodynamics, however, in the current paper we focus on the analytic results that can improve on Bjorken's famous initial energy density estimate. A more detailed, or a numerical hydrodynamical investigation is outside the scope of the present manuscript, however we can cross-check these results by fitting the simultaneously taken CMS and TOTEM data on $dn/d\eta$ with the same model, to investigate the stability of our initial energy density estimate from the details of $dn/d\eta$ at midrapidity.

7. Improved initial energy density using combined TOTEM+CMS $dN/d\eta$ data

Fit to TOTEM $dN/d\eta$ data was shown in Section 5 and in particular in Fig. 1. This shows an advanced estimate and reaches out to a large η region. However, it may seem necessary to put more attention on central η region and perform fits on a combined central+forward η region. Thus in this section we present $dN/d\eta$ distributions of charged particles from combined TOTEM+CMS datasets. In the left panel of Fig. 4 a fit to such combined data at 7 TeV [10,28] is shown.

This fit to TOTEM+CMS data [10,28] yields an initial flow acceleration parameter $\lambda = 1.076$ for 7 TeV pp collisions. As seen from the terms on the right hand side in Eq. (7), the corrected initial energy density depends on the acceleration parameter λ, the driving force for the hydrodynamic expansion or the pressure gradients and volume element expansion. Thus the advanced hydrodynamic estimate is

$$\epsilon_{\rm corr}(7\ {\rm TeV}) = 1.273 \times \epsilon_{\rm Bj}(7\ {\rm TeV}) = 0.645\ {\rm GeV/fm}^3. \tag{14}$$

Here we stress that compared to the $\epsilon_{\rm corr}$ estimate from fitting TOTEM only, the difference less than 1%, which is quite reasonable. The fit in the right panel of Fig. 4 shows the hydrodynamic

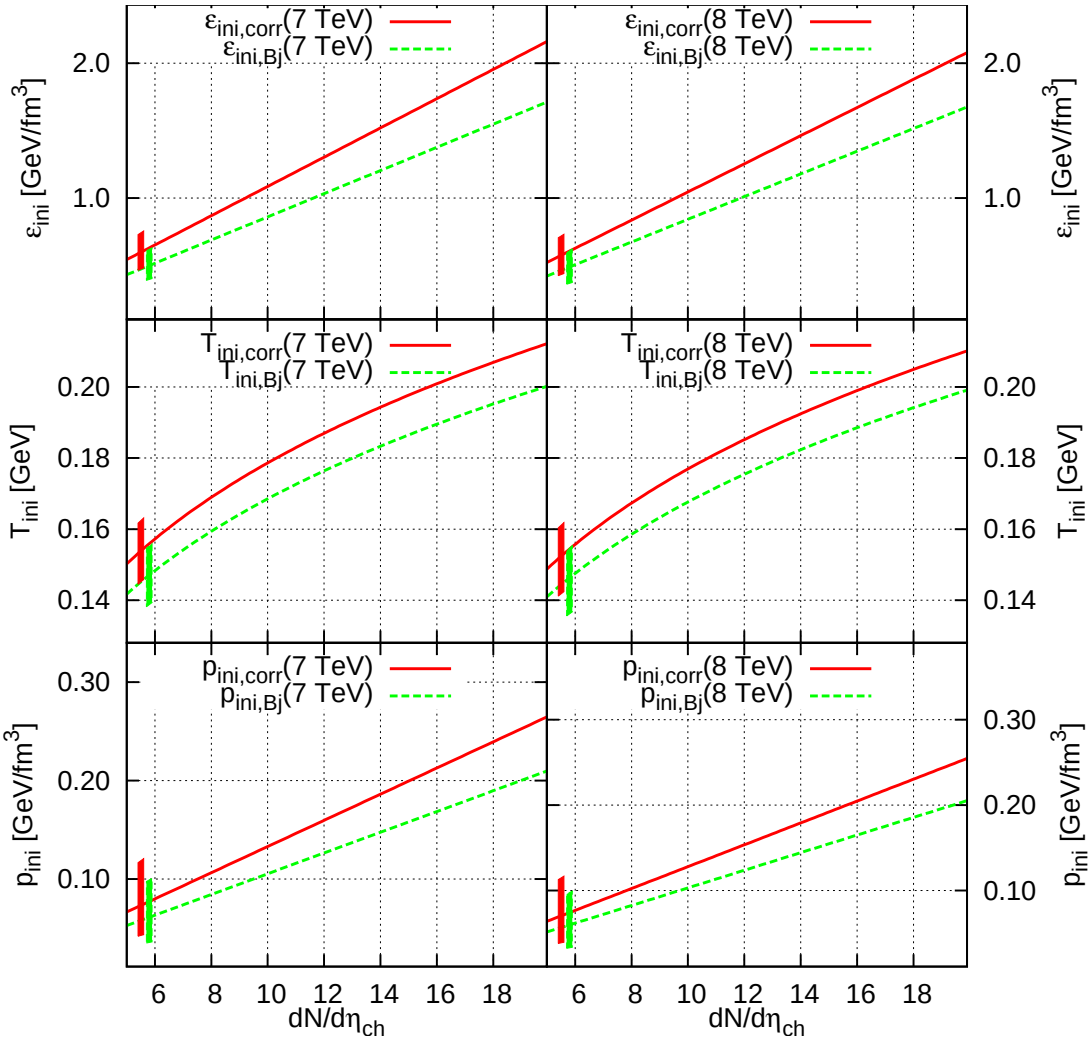

Figure 3. Initial energy density (based on Table 1), temperature and pressure (based on the $\epsilon \propto T^4$ relationship) at 7 TeV (left) and 8 TeV (right), is indicated as a function of central multiplicity density. The Bjorken-estimate (dashed curve) is above the critical energy density of 1 GeV/fm^3 if the multiplicity is larger than 12. Corrected initial energy density (solid curve) is above the critical value if multiplicity is larger than 9. Boxes (parallelograms) show systematic uncertainty (estimated from the 7 TeV case).

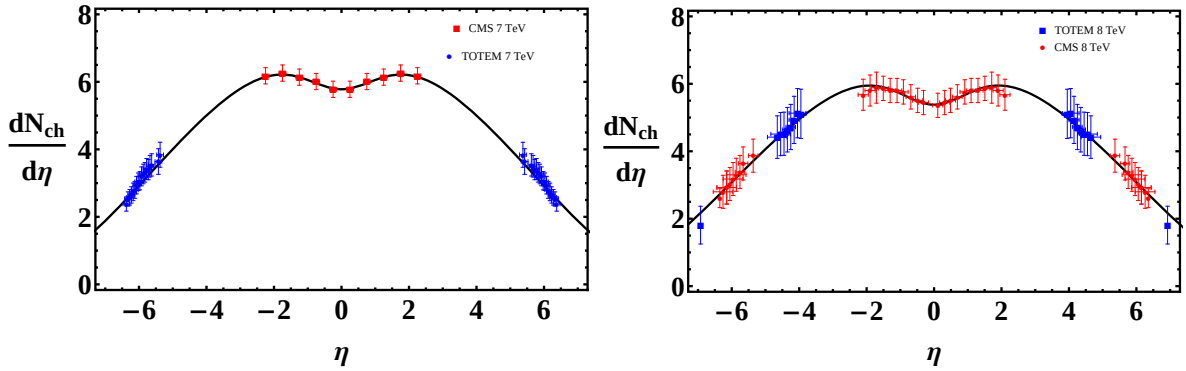

Figure 4. Left: Charged particle $\frac{dN}{d\eta}$ distributions from CMS [10] and TOTEM [28] at 7 TeV fitted with the result of our relativistic hydrodynamical solution described in this paper, with $\lambda = 1.076$. Right: Charged particle $\frac{dN}{d\eta}$ distributions from CMS and TOTEM 8 TeV data of Ref. [22,29] fitted with our results, with $\lambda = 1.066$.

$dN/d\eta$ distribution and charged particle in 8 TeV pp collision measured by TOTEM and CMS [22] (including TOTEM data measured in collisions with a displaced interaction vertex [29]). The resulting acceleration parameter is $\lambda = 1.066$, this corresponds to a final result of corrected initial energy density form the advance estimate

$$\epsilon_{\rm corr}(8\ {\rm TeV}) = 1.235 \times \epsilon_{\rm Bj}(8\ {\rm TeV}) = 0.641\ \ {\rm GeV/fm}^3 \tag{15}$$

which differs from the previous estimate based on only TOTEM data by less than 0.5%.

8. Summary

We have shown, that based on an accelerating hydro solution and data of the TOTEM and CMS experiments at CERN LHC, the advanced estimate of the initial energy density yields a value that below the critical value of 1 GeV/fm^3, but is not inconsistent with a supercritical state in high multiplicity 7 and 8 TeV proton-proton collisions. The energy density is proportional to the measured multiplicity, and so in high-multiplicity events, initial energy densities several times the critical energy density of 1 GeV/fm^3 have been reached. It means, that an important and necessary condition is satisfied for the formation of a non-hadronic medium in high multiplicity ($dn/d\eta_{\eta=0} > 9$) 7 and 8 TeV p+p collisions at CERN LHC, however, the exploration of additional signatures (radial and elliptic flow, volume or mean multiplicity dependence of the signatures of the nearly perfect fluid in p+p collisions, scaling of the HBT radii with transverse mass, and possible direct photon signal and low-mass dilepton enhancement) and their multiplicity dependence can be a subject of detailed experimental investigation even in p+p collisions at the LHC. It is also important to note, that even the measurement of differential elastic scattering cross-section has implications regarding this estimate.

We recall here that the application of hydrodynamical expansion to data analysis in high energy p+p collisions is not an unprecedented or new idea, as Landau worked out hydrodynamics for p+p collisions [30], and Bjorken also notes this possibility in his paper [7] describing his energy density estimate.

It is also noteworthy that Hama and Padula assumed [31] the formation of an ideal fluid of massless quarks and gluons in p+p collisions at CERN ISR energies of $\sqrt{s}$ = 53- 126 GeV. Alexopoulos et al. used Bjorken's estimate to determine the initial energy density of $\sim 1.1 \pm 0.2$ GeV/fm^3 at the Tevatron in $\sqrt{s}$ = 1.8 TeV p+$\overline{\rm p}$ collisions in the E735 experiment [32], while Lévai and Müller argued [33], that the transverse momentum spectra of pions and baryons indicate the creation of a fluid-like quark-gluon plasma in the same experiment at the same Tevatron energies. However, these earlier works considered the quark-gluon plasma as an ideal gas of massless quarks and gluons,

while the RHIC experiments pointed to a nearly perfect fluid of quarks where the speed of sound is measured to be $c_s \approx 0.35 \pm 0.05$ that is significantly different from that of a massless ideal gas of quarks and gluons, characterized by a $c_s = 1/\sqrt{3} \approx 0.57$. Recently, Shuryak and Zahed also proposed [34] the application of hydrodynamics for high multiplicity p+p and p+A collisions at CERN LHC.

The main result of our study indicates, that the initial energy density is apparently large enough in high multiplicity p+p collisions at the $\sqrt{s}$ = 7 and 8 TeV LHC energies to create a strongly interacting quark-gluon plasma, so a transition with increasing multiplicity is expected, as far as hydrodynamical phenomena are considered.

Probably the most important implication of our study is the need for an e+p and e+A collider: as far as we know only in lepton induced proton and heavy ion reactions can one be certain that a hydrodynamically evolving medium is not created even at the TeV energy range. The results of lepton-hadron and lepton-nucleus interactions thus will define very clearly the particle physics background to possible collective effects. For example, recently azimuthal correlations were observed in high multiplicity p+p and p+A as well as in heavy ion reactions (the ridge effect [35,36]), whose origin is currently not entirely clear. If such a ridge effect appears also in e+p and e+A collisions, then most likely this effect is not of a hydrodynamical origin, while if it does not appear in e+p and e+A collisions in the same multiplicity range as in p+p and p+A reactions, than the ridge is more likely a hydrodynamical effect.

If indeed a strongly interacting non-hadronic medium is formed in high multiplicity p+p collisions, than purely the jet suppression in heavy ion collisions does not reveal the true nature of these systems: the proper measure would be energy loss per unit length (as proposed in Ref. [37]), which may be quite similar in these systems, even if the total suppression is different.

We are looking forward to measurements unveiling the nature of the matter created in proton-proton collisions. In experimental p+p data, one should look for the enhancement of the photon to pion ratio in high multiplicity events (as compared to low multiplicity ones) [38], for a hydrodynamic scaling of Bose-Einstein correlation radii or that of azimuthal asymmetry [39], or even the enhancement of low mass dileptons [40].

Acknowledgments: The authors thank the important discussions to Simone Giani, Paolo Guibellino, Federico Antinori, Michael Tannenbaum, Péter Lévai, Sandra S. Padula, Endel Lippmaa and Renato Campanini. We acknowledge the support of the Hungarian OTKA grant NK-101438 and of the bilateral Chinese-Hungarian governmental project, TeT 12CN-1-2012-0016. T. Cs. gratefully acknowledges partial support from the Ch. Simonyi Foundation. M. Cs. was supported by the János Bolyai Research Scholarship of the Hungarian Academy of Sciences.

Bibliography

1. Adcox, K.; others., [**PHENIX Collaboration**]. Formation of dense partonic matter in relativistic nucleus nucleus collisions at RHIC: Experimental evaluation by the PHENIX collaboration. *Nucl. Phys.* **2005**, *A757*, 184–283, [arXiv:nucl-ex/0410003].
2. Csörgő, T.; Nagy, M.I.; Csanád, M. A New Family of Simple Solutions of Perfect Fluid Hydrodynamics. *Phys. Lett.* **2008**, *B663*, 306–311, [arXiv:nucl-th/0605070].
3. Csörgő, T.; Nagy, M.; Csanád, M. Accelerating Solutions of Perfect Fluid Hydrodynamics for Initial Energy Density and Life-Time Measurements in Heavy Ion Collisions. *Braz.J.Phys.* **2007**, *37*, 723–725, [arXiv:nucl-th/0702043].
4. Nagy, M.I.; Csörgő, T.; Csanád, M. Detailed description of accelerating, simple solutions of relativistic perfect fluid hydrodynamics. *Phys. Rev.* **2008**, *C77*, 024908, [arXiv:nucl-th/0709.3677].
5. Csörgő, T.; Nagy, M.; Csanád, M. New exact solutions of relativistic hydrodynamics. *J.Phys.G* **2008**, *G35*, 104128, [arXiv:nucl-th/0805.1562].
6. Hwa, R.C. Statistical Description of Hadron Constituents as a Basis for the Fluid Model of High-Energy Collisions. *Phys. Rev.* **1974**, *D10*, 2260.

7. Bjorken, J.D. Highly Relativistic Nucleus-Nucleus Collisions: The Central Rapidity Region. *Phys. Rev.* **1983**, *D27*, 140–151.
8. Bearden, I.G.; others., [**BRAHMS Collaboration**]. Pseudorapidity distributions of charged particles from Au + Au collisions at the maximum RHIC energy. *Phys. Rev. Lett.* **2002**, *88*, 202301, [nucl-ex/0112001].
9. Borsányi, S.; others. The QCD equation of state with dynamical quarks. *JHEP* **2010**, *11*, 077, [arXiv:hep-lat/1007.2580].
10. Khachatryan, V.; others., [**CMS Collaboration**]. Transverse-momentum and pseudorapidity distributions of charged hadrons in pp collisions at sqrt(s) = 7 TeV. *Phys.Rev.Lett.* **2010**, *105*, 022002, [arXiv:hep-ex/1005.3299].
11. Hofstadter, R. Electron scattering and nuclear structure. *Rev. Mod. Phys.* **1956**, *28*, 214–254.
12. Glauber, R.J.; Matthiae, G. High-energy scattering of protons by nuclei. *Nucl. Phys.* **1970**, *B21*, 135–157.
13. Block, M.M. Hadronic forward scattering: Predictions for the Large Hadron Collider and cosmic rays. *Phys. Rept.* **2006**, *436*, 71–215, [arXiv:hep-ph/hep-ph/0606215].
14. Antchev, G.; others., [**TOTEM Collaboration**]. Proton-proton elastic scattering at the LHC energy of s** (1/2) = 7-TeV. *Europhys.Lett.* **2011**, *95*, 41001, [arXiv:hep-ex/1110.1385].
15. Antchev, G.; others., [**TOTEM Collaboration**]. Luminosity-independent measurements of total, elastic and inelastic cross-sections at $\sqrt{s} = 7$ TeV. *Europhys.Lett.* **2013**, *101*, 21004.
16. Aamodt, K.; others., [**ALICE Collaboration**]. Charged-particle multiplicity measurement in proton-proton collisions at sqrt(s) = 7 TeV with ALICE at LHC. *Eur.Phys.J.* **2010**, *C68*, 345–354, [arXiv:hep-ex/1004.3514].
17. Aamodt, K.; others., [**ALICE Collaboration**]. Femtoscopy of pp collisions at sqrts=0.9 and 7 TeV at the LHC with two-pion Bose-Einstein correlations. *Phys.Rev.* **2011**, *D84*, 112004, [arXiv:hep-ex/1101.3665]. 21 pages, 18 figures.
18. Lacey, R.A.; others. Has the QCD critical point been signaled by observations at RHIC? *Phys. Rev. Lett.* **2007**, *98*, 092301, [arXiv:nucl-ex/0609025].
19. Csanád, M.; Májer, I. Equation of state and initial temperature of quark gluon plasma at RHIC. *Central Eur.J.Phys.* **2012**, *10*, 850–857, [arXiv:nucl-th/1101.1279].
20. Campanini, R.; Ferri, G.; Ferri, G. Experimental equation of state in proton-proton and proton-antiproton collisions and phase transition to quark gluon plasma. *Phys. Lett.* **2011**, *B703*, 237–245, [arXiv:hep-ph/1106.2008].
21. Adare, A.; others., [**PHENIX Collaboration**]. Enhanced production of direct photons in Au+Au collisions at $\sqrt{s_{NN}} = 200$ GeV and implications for the initial temperature. *Phys.Rev.Lett.* **2010**, *104*, 132301, [arXiv:nucl-ex/0804.4168].
22. Chatrchyan, S.; others., [**CMS Collaboration, TOTEM Collaboration**]. Measurement of pseudorapidity distributions of charged particles in proton-proton collisions at $\sqrt{s}$ = 8 TeV by the CMS and TOTEM experiments. *Eur.Phys.J.* **2014**, *C74*, 3053, [arXiv:hep-ex/1405.0722].
23. Adam, J.; others., [**ALICE Collaboration**]. Charged-particle multiplicities in proton-proton collisions at $\sqrt{s}$ = 0.9 to 8 TeV **2015**. [arXiv:nucl-ex/1509.07541].
24. Collaboration, C. Pseudorapidity and leading transverse momentum distributions of charged particles in pp collisions at 8 TeV. Technical report, 2013.
25. Antchev, G.; others., [**TOTEM Collaboration**]. Luminosity-Independent Measurement of the Proton-Proton Total Cross Section at $\sqrt{s} = 8$??TeV. *Phys.Rev.Lett.* **2013**, *111*, 012001.
26. Landau, L.D. On the multiparticle production in high-energy collisions. *Izv. Akad. Nauk SSSR Ser. Fiz.* **1953**, *17*, 51–64.
27. Bialas, A.; Janik, R.A.; Peschanski, R.B. Unified description of Bjorken and Landau 1+1 hydrodynamics. *Phys. Rev.* **2007**, *C76*, 054901, [arXiv:nucl-th/0706.2108].
28. Antchev, G.; others., [**TOTEM Collaboration**]. Measurement of the forward charged particle pseudorapidity density in pp collisions at $\sqrt{s} = 7$ TeV with the TOTEM experiment. *Europhys.Lett.* **2012**, *98*, 31002, [arXiv:hep-ex/1205.4105].
29. Antchev, G.; others., [**TOTEM Collaboration**]. Measurement of the forward charged particle pseudorapidity density in pp collisions at $\sqrt{s} = 8$ TeV using a displaced interaction point. *Eur. Phys. J.* **2015**, *C75*, 126, [arXiv:hep-ex/1411.4963].

30. Belenkij, S.Z.; Landau, L.D. Hydrodynamic theory of multiple production of particles. *Nuovo Cim. Suppl.* **1956**, *3S10*, 15.
31. Hama, Y.; Padula, S.S. Bose-Einstein correlation of particles produced by expanding sources. *Phys.Rev.* **1988**, *D37*, 3237.
32. Alexopoulos, T.; Anderson, E.; Bujak, A.; Carmony, D.; Erwin, A.; others. Evidence for hadronic deconfinement in anti-p - p collisions at 1.8-TeV. *Phys.Lett.* **2002**, *B528*, 43–48, [arXiv:hep-ex/hep-ex/0201030].
33. Lévai, P.; Müller, B. Transverse baryon flow as possible evidence for a quark - gluon plasma phase. *Phys.Rev.Lett.* **1991**, *67*, 1519–1522.
34. Shuryak, E.; Zahed, I. High Multiplicity pp and pA Collisions: Hydrodynamics at its Edge and Stringy Black Hole **2013**. [arXiv:hep-ph/1301.4470].
35. Chatrchyan, S.; others., [**CMS Collaboration**]. Observation of long-range near-side angular correlations in proton-lead collisions at the LHC. *Phys.Lett.* **2013**, *B718*, 795–814, [arXiv:nucl-ex/1210.5482].
36. Padula, S.S., [**CMS Collaboration**]. Long-range dihadron correlations in high multiplicity p p and PbPb with CMS. *PoS* **2011**, *WPCF2011*, 023.
37. Csörgő, T. Critical Opalescence: An Optical Signature for a QCD Critical Point. *PoS* **2009**, *CPOD2009*, 035, [arXiv:nucl-th/0911.5015].
38. Tannenbaum, M.J.; Weiner, R.M. Comments on 'Observation of Long-Range, Near-Side Angular Correlations in Proton-Proton Collisions at the LHC' by the CMS collaboration **2010**. [arXiv:hep-ph/1010.0964].
39. Adare, A.; others., [**PHENIX Collaboration**]. Scaling properties of azimuthal anisotropy in Au + Au and Cu + Cu collisions at s(NN)**(1/2) = 200-GeV. *Phys. Rev. Lett.* **2007**, *98*, 162301, [arXiv:nucl-ex/0608033].
40. Afanasiev, S.; others., [**PHENIX Collaboration**]. Enhancement of the dielectron continuum in s(NN)**(1/2) = 200-geV Au+Au collisions **2007**. [arXiv:nucl-ex/0706.3034].